Title: Transcriptional response to West Nile virus infection in the zebra finch (*Taeniopygia guttata*), a songbird model for immune function

Authors:
Daniel J Newhouse[1*], Erik K Hofmeister[2], Christopher N Balakrishnan[1]

[1] Howell Science Complex, East Carolina University, Greenville, North Carolina, 27858, USA
[2] U.S. Geological Survey, National Wildlife Health Center, 6006 Schroeder Road, Madison, Wisconsin 53711, USA
[*] Corresponding Author: newhoused12@students.ecu.edu

West Nile Virus (WNV) is the one of most widespread arboviruses worldwide. WNV exists in a bird-mosquito transmission cycle where passerine birds act as the primary reservoir host. As a public health concern, the mammalian immune response to WNV has been studied in detail. Little, however, is known about the avian immune response to WNV. Avian taxa show variable susceptibility to WNV and what drives this variation is unknown. Thus, to study the immune response to WNV in birds, we experimentally infected captive zebra finches (*Taeniopygia guttata*). Zebra finches provide a useful model, as like many natural avian hosts they are moderately susceptible to WNV and thus provide sufficient viremia to infect mosquitoes. We performed splenic RNAseq during peak viremia to provide an overview of the transcriptional response. In general, we find strong parallels with the mammalian immune response to WNV, including up-regulation of five genes in the Rig-I-like receptor signaling pathway, and offer insights into avian specific responses. Together with complementary immunological assays, we provide a model of the avian immune response to WNV and set the stage for future comparative studies among variably susceptible populations and species.

Introduction:

West Nile virus (WNV) is a single-stranded RNA flavivirus that exists in an avian-mosquito transmission cycle, where birds (typically Passeriformes) act as the primary amplification hosts. In addition to birds, nearly 30 other non-avian vertebrate species have been documented as hosts (1). Although many WNV-infected hosts are asymptomatic, WNV infection can cause severe meningitis or encephalitis in those that

40 are highly susceptible. Avian species for the most part exhibit low to moderate
41 susceptibility. That is, individuals become infected and develop sufficient viremia for
42 transmission via mosquito blood meal, but the hosts recover and avoid significant
43 mortality, reviewed in (2). First described in 1937, WNV has not resulted in widespread
44 avian decline throughout its historical range (3), perhaps due to host-parasite coevolution.
45 However, the emergence of WNV in North America in 1999 has negatively impacted a
46 wide range of populations (4,5). Surveys of North American wild birds have shown a
47 variety of competent WNV hosts, with varying degrees of susceptibility, morbidity, and
48 pathogenicity (2). American robins (*Turdus migratorius*) appear to be the main host in
49 spreading WNV infection in North America (6), but infection appears most detrimental to
50 members of Family Corvidae (7). Despite great variation in susceptibility, the
51 mechanisms underlying this variation are primarily unknown (2).
52
53 Largely due to interest in human health implications, most work describing the
54 host immune response to WNV infection has been performed in mammalian systems (8).
55 From these studies, we know that in mammals, both the innate and adaptive arms are
56 critical for virus detection and clearance (9,10). Within the innate immune response, the
57 retinoic acid-inducible gene 1(Rig-I)-like receptor (RLR) pathway appears to play a key
58 role in viral clearance. This pathway recognizes viral products and initiates type I
59 interferon expression (11). Mice lacking the viral recognition RLR genes in this pathway,
60 DDx58 (Rig-I) and IFIH1 (MDA5), become highly susceptible to WNV infection (12). In
61 the adaptive immune system, a broad range of components appear to play important roles
62 in mounting a response, including antibody and CD4+ and CD8+ T cells (9,13,14).

63 Interestingly, major histocompatibility complex (MHC) class I genes are up-regulated
64 post-infection (15,16). Viruses typically evade MHC class I detection (17,18), as MHC
65 class I molecules bind and present viral peptides to CD8+ T cells. However, the purpose
66 of WNV induced MHC expression is unclear.
67
68 While the mammalian immune response to WNV infection has been extensively
69 studied, the avian immune response remains mostly unknown. Of the studies in birds,
70 many involve experimentally infecting wild caught birds, reviewed in (2), or domestic
71 chickens (*Gallus gallus*) (19). These studies primarily focus on viral detection, tissue
72 tropism, antibody production, or lymphocyte counts (2,19,20). Little is known about the
73 molecular mechanisms driving the immune response to WNV infection, but see (21).
74 Furthermore, current avian WNV studies suffer many challenges. Wild caught birds may
75 be co-infected with other parasites (e.g. avian malaria) and are difficult to maintain in
76 captivity for experimental infection studies. Chickens, although an avian model species,
77 are highly resistant to WNV infection (22), uncommon hosts, and therefore are not ideal
78 to describe the avian immune response to WNV infection. Passeriformes and Galliformes
79 are also highly divergent bird lineages, with distinctive immune gene repertoires and
80 architecture (23).
81
82 As passerine birds are the main hosts for WNV, we have sought to develop a
83 passerine model to study the impacts of WNV infection on a taxonomically appropriate
84 host (24). We have recently shown that zebra finches, *Taeniopygia guttata,* are
85 moderately susceptible hosts for WNV (25). That is, WNV rapidly disseminates to a

86 variety of tissues and is detectable in most samples by four days post-inoculation (dpi).
87 Despite rapid development of sufficient viremia for arthropod transmission, zebra finches
88 develop anti-WNV anitbodies, clear WNV by 14dpi, and avoid significant mortality (25).
89 This moderate disease susceptibility is similar to what is observed in many natural WNV
90 hosts. Zebra finches are also an established biomedical model system with a suite of
91 genetic and genomic tools available (26).
92
93 In this study, we experimentally infected zebra finches and performed splenic
94 RNAseq to describe their transcriptional response over the time course of infection. In
95 doing so, we characterize the zebra finch immune response to WNV infection, explore
96 expression of the avian RLR pathway in response to WNV, gain insights into the avian
97 immune response to this widespread infectious disease, and uncover conserved
98 evolutionary responses in avian and mammalian systems.
99
100 **Results**
101 *Experimental infection*
102 We challenged six individuals with with 10^5 plaque forming units (PFU) WNV
103 and sequenced RNA (Illumina RNAseq) isolated from spleens, an organ critical to the
104 avian immune response. Three birds served as procedural controls and on day 0 were
105 injected subcutaneously with 100 µL of BA1 media, as previously described (27).
106 Peak viremia occurrs at 4.6 ±1.7 dpi as quantified via RT-PCR (25) and thus, we
107 characterized the transcriptional response leading to (2dpi, n=3) and at peak viral load
108 (4dpi, n=3) in the present study. WNV RNA was detected by culture in lung and kidney

109 RNA pools of 2 out of 3 birds sampled at day 2, and all 3 birds sampled at 4dpi. These
110 findings were verified by semi-quantitative RT-PCR. Because WNV is rarely detected in
111 spleen by 2dpi, but all birds previously inoculated at 10^5 PFU developed WNV antibodies
112 [25] we treated all six birds inoculated with WNV as being infected.
113
114 *Sequencing results & read mapping*
115 We obtained 18-30 million paired-end, 100bp reads for each sample and removed
116 0.57-1.24% of the total bases after adapter trimming (Supplementary Table S1). On
117 average, 79.0-80.8% total trimmed reads mapped to the zebra finch reference genome
118 (Supplementary Table S2), corresponding to 18,618 Ensembl gene IDs. Of these, 14,114
119 genes averaged at least five mapped reads across all samples and were utilized for
120 differential expression (DE) analyses.
121
122 *Sample clustering & differential expression*
123 We tested for DE two ways: as pairwise comparisons between treatments to
124 identify specific genes with *DEseq2* (28) and as a time-course grouping genes into
125 expression paths with *EBSeqHMM* (29). To visualize patterns of expression variation
126 among samples, we conducted principal component analysis (PCA) and distance-based
127 clustering (Supplemental Figures S1 & S2). The first three principal components
128 explained 93.04% of the variance in gene expression, but none of the PCs were
129 significantly correlated with treatment (ANOVA, PC1: $p = 0.288$, PC2: $p = 0.956$, PC3: p
130 $= 0.202$). Although this finding suggests that much of the expression variation was

131 independent of the experimental treatment, pairwise comparisons revealed genes that
132 were DE between treatments.
133
134 When comparing Control vs. 2dpi, we found 161 differentially expressed genes
135 (adjusted $p < 0.10$, average $\log_2$ fold-change (FC) = 1.74). This gene list includes several
136 immune related genes associated with the innate (e.g. IL18) and adaptive (e.g. MHC IIB)
137 immune system (Table 1, Figure 1). Sixty-five genes were differentially expressed
138 between Control and 4dpi (average $\log_2$FC = 1.61), also with several immune relevant
139 genes including five genes in the RLR pathway (Table 1, Figure 2, Figure 3). Lastly, we
140 observed 44 DE genes between 2dpi vs. 4dpi individuals (average $\log_2$FC = 1.56). Three
141 of these have described functions in immunity. The complete list of *DEseq2* DE genes
142 (adjusted $p < 0.10$) across all comparisons can be found in Supplementary Table S3 and
143 immune relevant DE genes are listed in Table 1 along with their gene name, $\log_2$ fold
144 change, padj value, and comparison to mammalian studies. We also combined 2dpi and
145 4dpi cohorts and compared with control, but due to high variation in gene expression
146 between days 2 and 4 dpi, we only found 16 DE genes (average $\log_2$FC = 1.64) between
147 Control and Infected cohorts, one of which was associated with immunity.
148
149 When analyzed for DE as a time course in *EBSeqHMM*, 686 genes showed
150 evidence of differential expression (posterior probability > 0.99, FDR < 0.01). Most DE
151 genes (n = 561) were suppressed following infection ("Down-Down") or varied between
152 conditions. Seventy-five genes were "Up-Down", 49 were "Down-Up" and 1 was "Up-
153 Up". As expected, we found overlap of several immune genes between the two analyses.

For example, IL18, APOD and IFITM10 are “Up-Down" (Supplementary Table S5) and this trend is reflected in the *DEseq2* Control vs 2dpi analysis (Figure 1).

Functional annotation of differentially expressed genes

To place differentially expressed genes into groups based on their biological function, we performed a gene ontology (GO) analysis using the *GOfinch* tool (30). As above, we conducted GO analyses based on multiple pairwise analyses of gene expression. The strongest evidence of functional enrichment was observed in the contrast of Control vs. 4dpi. This list of 65 differentially expressed genes showed functional enrichment of 55 GO terms (Fisher’s Exact Test, FDR $p < 0.05$ (Benjamini Hochberg method [31])). It is in this contrast where the immune response manifests itself most strongly, with a large list of immune-related categories (Supplementary Table S4) and a broad range of immune functioning genes differentially expressed (n=14, Tables 1 & 2). When comparing genes differentially expressed between Control and 2dpi, only one GO category was strongly enriched (“integral to membrane”, expected = 15, observed = 35, $p = 0.00065$). In this contrast we also observed several slightly enriched immune related GO categories such as “inflammatory response” and “negative regulation of T cell migration” but these fall outside of our significance threshold (Supplementary Table S4) and reflect only few genes (e.g. APOD and IL18) that were DE in the Control vs. 2dpi analysis. A set of 57 enriched GO categories describe genes DE between 2 and 4dpi. Although some of these involved T and B cell regulation, these categories were also only represented by a single gene each (ADA) (Table 2, Supplementary Table S4). We found

no evidence of functional enrichment among DE genes between Control vs. Infected (2dpi and 4dpi) cohorts.

We also conducted a similar analysis of genes identified as DE by *EBseqHMM*, which revealed two (Up-Up), 107 (Up-Down), 12 (Down-Up) and 73 (Down-Down) significantly enriched GO categories (adjusted $p < 0.05$, Supplementary Table S5). Interestingly, Up-Down GO categories had the strongest representation of immune related GO terms, including "cytokine receptor activity" (expected = 0, observed = 3 p = 0.015) and "positive regulation of interferon-gamma production" (expected = 0, observed = 2, p = 0.028). However, we also observed a strong immune signature among Down-Down Genes (GO Term "Immune Response", expected = 3, observed = 11, p = 0.013), which represents several innate immune genes including three complement genes and interferon gamma. Twelve categories were significantly enriched among "Down-Up" genes, including "double-stranded RNA binding" (expected = 0, observed = 2, adjusted p = 0.049). One of the observed genes in this category is OASL, which has been demonstrated to have antiviral activity towards WNV in chickens (21). Lastly, as in the *DEseq2*-based analysis, we also detected a strong enrichment signature of membrane proteins. Genes annotated as "integral to membrane" were highly enriched among those showing an Up-Down pattern (expected = 6, observed =14, adjusted $p < 0.028$, Supplementary Table S5). Combined, we find broad overlap in GO representation between the *EBseqHMM* and *DEseq2* approaches.

198 In addition to placing genes into broad systematic functions in the GO analysis,
199 we were also interested in placing our gene expression results in the context of immune
200 pathways of interest. The RLR antiviral pathway is critical to WNV clearance in
201 mammals (12) and appears important in mounting an immune response to avian influenza
202 in ducks (32-34). Utilizing *Pathview v1.8.0* (35), we find that WNV infection induces the
203 RLR pathway. Five genes, including the two RLR genes, DDx58 and IFIH1, which
204 encode the Rig-I and MDA5 viral detection molecules, are significantly up-regulated
205 (Table 1, Figure 3, Supplementary Figure S3). We detect expression of 36/37 genes in the
206 pathway, many of which are also up-regulated, though not always significantly.
207
208 *De novo transcriptome analysis*
209 To reveal any genes responding to infection missed by our genome based
210 analysis, we created a reference transcriptome with *Trinity v2.1.1* (35) and annotated
211 against the NCBI non-redundant database with *DIAMOND*, a *BLASTx*-like aligner (37).
212 Our *de novo* transcriptome assembly resulted in 393,408 *Trinity* transcripts. We
213 visualized our annotated transcriptome with *MEGAN* (38), which places genes into
214 KEGG pathways. In doing so, we confirmed many expression results from the genome-
215 based approach and importantly, this analysis revealed expression of two transcripts with
216 homology to interferon alpha, which was absent (but annotated) in the genome based
217 analysis described above. Combined, our genome-based and reference-free approaches
218 detect regulation of the complete RLR pathway in zebra finches.
219
220 **Discussion**

We have characterized the zebra finch transcriptional response to WNV infection. Overall, we find that as in mammalian systems, components of both the adaptive and innate immune pathways are activated following infection. While WNV is primarily an avian specific infectious disease, most work describing the host immune response to infection has been performed in mammals. Despite genomic, physiological and evolutionary differences between birds and mammals, the host immune response shows broad similarity between taxa (Table 1).

We were particularly interested in the role of the innate RLR pathway. This pathway mounts an antiviral innate immune response and is critical for WNV detection and clearance in mammals (12). By combining genome and transcriptome-based approaches, we show here that the RLR pathway in zebra finches is induced by WNV infection, as gene expression is detected throughout the pathway. Furthermore, five genes in this pathway are significantly up-regulated at 4dpi (Figure 3, Supplementary Figure S3), including IFIH1 and DDx58 (Figure 2B), which encode molecules that recognize WNV particles in mammals (39). This results in a corresponding over-representation of genes in the RLR pathway GO categories (Table 2). While no studies have investigated the role of the RLR following WNV infection in birds, this pathway appears important for avian influenza clearance in ducks (32-34), Buggy Creek virus clearance in house sparrows (39), and likely for the broad avian antiviral immune response, including WNV.

We observed other parallels with mammals as well (Table 1). For example, T-Cell Immunoglobulin Mucin Receptor 1 (TIM1) is up-regulated at 2dpi in zebra finches

(Figure 1A, C). In human cell lines, expression of TIM1 promotes infection of WNV virus like particles (VLPs) (41,42), suggesting that the up regulation of TIM1 seen in zebra finches may promote viral entry as well. Similarly, C-C motif chemokine (ENSTGUG00000005295) is up-regulated in our study at 2dpi and in previous human cell line and mouse experiments, suggesting a conserved role in chemokine production following WNV infection (43-45). Apolipoprotein D (APOD), a gene typically involved in brain injury and potentially responding to the neurodegenerative nature of WNV, is up-regulated in WNV infected mice (46), as well as in our study. Two interferon stimulated genes (ISGs), ADAR and MOV10 are both significantly up-regulated at 4dpi relative to control. Schoggins et al. (47) showed ADAR expression to enhance WNV replication and MOV10 expression to have antiviral activity. While further testing of these genes is needed to validate their roles in avian WNV infection, they nonetheless offer insights into a broad range of conserved responses between mammals and birds.

Within the adaptive immune response, the role of the MHC in the host response to WNV is also particularly interesting. The MHC plays a key role in antigen processing and presentation. The MHC comprises two main classes (Class I & II) and both are up-regulated in mammals following WNV infection (48,15,16). Similarly, two genes encoding MHC class IIB proteins are significantly up-regulated in zebra finches at 2dpi (Figure 1). Unlike mammals, however, we found that MHC class I is not significantly DE in any comparison. In mammals, upregulation of MHCI may not be adaptive for the host, as upregulation may actually be a mechanism by which the virus evades Natural Killer (NK) cell detection by the innate immune system (15). It has also been suggested that

MHC up-regulation is a byproduct of flavirus assembly (49). Interestingly, at 2dpi, interleukin-18 (IL18) is significantly up- regulated (Table 1, Figure1A,B). IL18 can enhance NK cell activity (50) and is potentially a mechanism by which the immune system can counteract WNV evasion strategies via NK cell activation, although further testing is needed to quantify NK cell activity in zebra finches to support this hypothesis.

Despite many similarities, several immune genes differentially expressed in our analyses have not been previously reported in the mammalian WNV literature or are expressed differently in zebra finches (Table 1). For example, at 2dpi, the proinflammatory cytokine IL18 was significantly up-regulated in zebra finches (Figure 1), contrasting a previous study in human cell lines, which show no difference in IL18 expression following WNV infection (50). Furthermore, interferon regulatory factor 6 (IRF6) was down-regulated at 2dpi, but up-regulated in human macrophages following infection (43). Another significantly down-regulated gene at 2dpi, ubiquitin carboxyl-terminal hydrolase L1 (UCHL1), has been shown to suppress cellular innate immunity in human cell lines infected with high-risk human papilloma virus (52). Down-regulation restores functional pattern recognition receptor (PRR) pathways (e.g. RLR). The down-regulation of UCHL1 here thus is associated with the previously described regulation of the PRR RLR pathway in this study (Table 1). Lastly, interferon-induced protein with tetratricopeptide repeats (IFIT) and interferon-inducible transmembrane proteins (IFITM) gene families are known innate antiviral proteins and have been shown to restrict WNV entry in human cells lines (47, 53). Both IFIT5 and IFITM10 are up-regulated (Figure 2A,C) in our study and yet, to our knowledge, neither have previously been implicated in

290 the host immune response to WNV. This potentially reveals an avian specific function of
291 IFIT5 and IFITM10.
292
293 Like many passerine birds infected in nature, zebra finches are moderately
294 susceptible to WNV, developing sufficient viremia to serve as competent hosts, but
295 generally resisting mortality due to infection (25). While there are clear differences
296 among treatments in terms of differentially expressed genes (Table 1), the weak effect of
297 treatment on overall expression profile (Supplemental Figure S1 & S2). may be a
298 reflection of this moderate susceptibility. Most zebra finches are able to clear WNV
299 inflection by 14 dpi (25). In pairwise comparisons, there are between 16 and 161
300 differentially expressed genes, depending on the treatment comparison (Supplementary
301 Table S3). WNV infection intensity varies among tissues (20), but due to the spleen's
302 important role in the avian immune system (54,55), we expect these results to be
303 representative of the overall immune response.
304
305 Functional enrichment of several immune GO terms primarily appears in Up-
306 Down path defined by *EBseqHMM* (Supplementary Table S5), as many genes in the
307 immune system are up-regulated post-infection, as also seen in the *DEseq2* analysis
308 (Table 1, Figure 1, Figure 2). In both the *EBseqHMM* and *DEseq2* analyses, most of the
309 significant immune GO categories are innate immune responses, although adaptive
310 immune categories involved in B/T cell proliferation appear in both (Table 2,
311 Supplementary Tables S4 & S5). Similar to the mammalian model, broad organismal

312 processes, encompassing the entire immune response, are represented in the zebra finch
313 response to WNV.
314
315 The zebra finch was the second bird to have its genome sequenced (26). However,
316 the zebra finch genome assembly and gene annotation remain incomplete. Immune genes
317 in particular are difficult to reconstruct in genomes due to their complex evolutionary
318 history (e.g. MHC, [23]). Our mapping results indicated that roughly 80% of our reads
319 mapped to the genome. While the unmapped 20% could contain poor quality reads or
320 non-avian sequences, it also represents zebra finch reads that could not be appropriately
321 mapped to the reference. Thus, we took a genome-independent approach and assembled a
322 *de novo* zebra finch transcriptome from our nine paired-end samples. Interestingly, RLR
323 induced interferon expression was not detected in the genome-based analysis. The
324 transcriptome analysis, however, revealed expression of two transcripts with homology to
325 interferon alpha, thus completing the pathway from virus detection to interferon
326 production.
327
328 We have begun to develop the zebra finch as an avian model for the host response
329 to WNV infection. We show here that the zebra finch immune response is largely
330 conserved with that seen in mammalian-based studies (Table 1). Additionally, we
331 identify many components of the immune system that have not been previously
332 implicated in the host immune response to WNV. This potentially reveals an avian-
333 specific immune response and highlights avenues for future research. Combined with our
334 recent immunological characterization (25), we have broadly described the immune

response of a moderately susceptible avian host for WNV. This sets the stage for future comparative work to uncover the genetic basis of variable avian susceptibility to WNV infection.

Methods

Experimental Setup

All animal use was approved by the USGS National Wildlife Health Center Institutional Animal Care and Use Committee (IACUC Protocol: EP120521) and this study was performed in accordance with USGS IACUC guidelines. The experimental infection setup is described in detail in (25). Briefly, nine female zebra finches were randomly divided into three cohorts, one unchallenged and two challenged (n = 3 each). Birds were challenged subcutaneously with 100ul BA1 media containing 10^5 plaque-forming units (PFU) of the 1999 American crow isolate of WNV (NWHC 16399-3) and sacrificed at 2 and 4 dpi, corresponding to peak viremia. Uninfected individuals were injected with 100ul BA1 media and sacrificed at 4dpi. WNV infection was confirmed by RT-PCR, as previously described (26), in lung and kidney pooled tissue (25). Spleens from each individual were removed, placed into RNAlater (Qiagen, Valencia, CA USA), and frozen at -80 °C until RNA extraction.

RNA extraction & sequencing

Whole spleen tissue was homogenized in Tri-Reagant (Molecular Research Company) and total RNA was purified with a Qiagen RNeasy (Valencia, CA USA) mini kit following the manufacturer's protocol. RNA was DNAse treated and purified.

Purified RNA was quality assessed on a Bioanalyzer (Agilent, Wilmington, DE USA) to ensure RNA quality before sequencing (RIN = 6.6-8.1). All library prep and sequencing was performed at the University of Illinois Roy J. Carver Biotechnology Center. A library for each sample was prepared with an Illumina TruSeq Stranded RNA sample prep kit. All libraries were pooled, quantitated by qPCR, and sequenced on one lane of an Illumina HiSeq 2000 with a TruSeq SBS Sequencing Kit producing paired-end 100nt reads. Reads were analyzed with Casava 1.8.2 following manufacturer's instructions (Illumina, San Diego, CA). Sequencing data from this study have been deposited in the NCBI Sequence Read Archive (BioProject: PRJNA352507).

Adapter trimming & read mapping

We removed Illumina adapters from reads with *Trim Galore! v0.3.7* (http://www.bioinformatics.babraham.ac.uk/projects/trim_galore/) which makes use of *Cutadapt v1.7.1* (56). Reads were then mapped to the zebra finch genome (*v3.2.74*,6) using *TopHat v2.0.13* (57), which utilizes the aligner *Bowtie v2.2.4* (58). We specified the library type as fr-firststrand in *TopHat2*. Successfully mapped reads were converted from SAM to BAM format with *SAMtools View v1.2* (59,60) and counted in *htseq-count v0.6.0* specifying '-s rev' (61). This assigned zebra finch Ensembl gene IDs and we only retained genes that mapped an average of five times across each sample.

Differential expression

Gene counts were then normalized for read-depth and analyzed for DE in *DEseq2 v1.8.1* (28). We analyzed DE across four comparisons: Control vs. Infected, Control vs.

2dpi, Control vs. 4dpi, and 2dpi vs. 4dpi. We visualized expression profiles in *R v3.3.0* (62) by PCA with the R package pcaExplorer (63), and hierarchical clustering heat maps with the ggplot2 library (64) following the *DEseq2* manual. *DEseq2* tests for DE with a Wald test and genes were considered differentially expressed if the Benjamini & Hochberg (31) false discovery rate (FDR) correction for multiple testing p value < 0.10. We chose this significance threshold as *DEseq2* is generally conservative in classifying DE (65). Furthermore, this cutoff has been used in other RNAseq experimental infection studies (66). We plotted genes of interest individually with the plotCounts function in *DEseq2* and clustered expression profiles of these genes with the pheatmap R library to view expression levels across samples and treatments.

We tested DE genes for under and over representation of gene ontology (GO) categories with the *CORNA* software (http://www.ark-genomics.org/tools/GOfinch, [30]). Significant DE genes were tested against all genes in our dataset. Statistical significance was determined using Fisher's exact tests corrected for multiple hypothesis testing ($p < 0.05$). To visualize DE results in the context of the RLR pathway, we utilized *Pathview v1.8.0* (35) to plot the log fold change of each gene detected in our dataset into the Kyoto Encyclopedia of Genes and Genomes (KEGG) pathway (KEGG ID = 04622) (67,68).

Time-course gene expression

In addition to the pair-wise comparisons performed in *DEseq2*, we were interested in understanding how clusters of genes are differentially expressed over the time course of infection. Thus, we performed DE analyses in *EBSeqHMM* (29). *EBSeqHMM* utilizes

a bayesian approach with a hidden Markov model to identify DE between ordered conditions. Genes are then grouped into expression paths (i.e. "Up-Down", "Down-Down"), in which DE occurs when expression paths change between at least one adjacent condition. For example, a gene up-regulated at both 2dpi relative to control and 4dpi relative to 2dpi would be classified as "Up-Up". We included three time points, with control individuals classified as t1, 2dpi as t2 and 4dpi as t3. Genes were considered DE at posterior probability > 0.99 and FDR < 0.01. We chose a more stringent cutoff in this analysis as *EBseq* can be liberal in classifying differential expression (65) and based on visual inspection of expression profiles. Using genes identified as DE we performed the GO analysis described above.

De novo transcriptome analysis

The use of Ensembl gene annotations for read counting restricts analyses to previously annotated genes. To test for potential regulation in any unannotated genes, we created a *de novo* transcriptome from our trimmed, paired-end reads using *Trinity v2.0.6* (36). We used default Trinity parameters with the exception of server specific settings (e.g. --max_memory 100G) and strand specificity (--SS_lib_type RF). To annotate our transcriptome, we used the *BLASTX*-like aligner *DIAMOND v0.7.11* (37), which utilizes NCBI's non redundant database. We visualized results in *MEGAN v5.10.6* (38), which places transcripts into functional pathways (e.g. KEGG), facilitating comparisons to our genome based analysis.

References

1. Chancey, C., Grinev, A., Volkova, E. & Rios, M. The Global Ecology and Epidemiology of West Nile Virus. *Biomed Res. Int.* 2015, 20 (2015).

2. Pérez-Ramírez, E., Llorente, F. & Jiménez-Clavero, M. Á. Experimental infections of wild birds with West Nile virus. *Viruses* 6, 752–781 (2014).

3. McLean, R. G. *et al.* West Nile virus transmission and ecology in birds. *Ann N Y Acad Sci* 951, 54–57 (2001).

4. LaDeau, S. L., Kilpatrick, a M. & Marra, P. P. West Nile virus emergence and large-scale declines of North American bird populations. *Nature* 447, 710–713 (2007).

5. George, T. L. *et al.* Persistent impacts of West Nile virus on North American bird populations. *Proc. Natl. Acad. Sci. U. S. A.* 1507747112– (2015).

6. Kilpatrick, a M., Daszak, P., Jones, M. J., Marra, P. P. & Kramer, L. D. Host heterogeneity dominates West Nile virus transmission. *Proc. Biol. Sci.* 273, 2327–2333 (2006).

7. Komar, N. *et al.* Experimental infection of North American birds with the New York 1999 strain of West Nile virus. *Emerg. Infect. Dis.* 9, 311–322 (2003).

8. Suthar, M. S., Diamond, M. S. & Gale, M. West Nile virus infection and immunity. *Nat. Rev. Microbiol.* 11, 115–28 (2013).

9. Diamond, M. S., Shrestha, B., Mehlhop, E., Sitati, E. & Engle, M. Innate and adaptive immune responses determine protection against disseminated infection by West Nile encephalitis virus. *Viral Immunol.* 16, 259–278 (2003).

10. Diamond, M., Shrestha, B. & Marri, A. B cells and antibody play critical roles in the immediate defense of disseminated infection by West Nile encephalitis virus. *J. Virol.* 77, 2578–2586 (2003).

11. Diamond, M. S. & Gale, M. Cell-intrinsic innate immune control of West Nile virus infection. *Trends Immunol.* 33, 522–530 (2012).

12. Errett, J. S., Suthar, M. S., McMillan, A., Diamond, M. S. & Gale, M. The essential, nonredundant roles of RIG-I and MDA5 in detecting and controlling West Nile virus infection. *J. Virol.* 87, 11416–25 (2013).

13. Sitati, E. M. & Diamond, M. S. CD4+ T-cell responses are required for clearance of West Nile virus from the central nervous system. *J. Virol.* 80, 12060–12069 (2006).

14. Shrestha, B. & Diamond, M. Role of CD8+ T cells in control of West Nile virus infection. *J. Virol.* 78, 8312–8321 (2004).

15. Lobigs, M., Müllbacher, A. & Regner, M. MHC class I up-regulation by flaviviruses: Immune interaction with unknown advantage to host or pathogen. *Immunol. Cell Biol.* 81, 217–223 (2003).

16. Cheng, Y., King, N. J. C. & Kesson, A. M. Major histocompatibility complex class I (MHC-I) induction by West Nile virus: involvement of 2 signaling pathways in MHC-I up-regulation. *J. Infect. Dis.* 189, 658–668 (2004).

17. Hewitt, E. W. The MHC class I antigen presentation pathway: strategies for viral immune evasion. *Immunology* 110, 163–169 (2003).

18. Petersen, J. L., Morris, C. R. & Solheim, J. C. Virus evasion of MHC class I molecule presentation. *J. Immunol.* 171, 4473–4478 (2003).

19. Fair, J. M., Nemeth, N. M., Taylor-McCabe, K. J., Shou, Y. & Marrone, B. L. Clinical and acquired immunologic responses to West Nile virus infection of domestic chickens (*Gallus gallus domesticus*). *Poult. Sci.* 90, 328–336 (2011).

20. Gamino, V. & Höfle, U. Pathology and tissue tropism of natural West Nile virus infection in birds: A review. *Vet. Res.* 44, (2013).

21. Tag-El-Din-Hassan, H. T. *et al.* The chicken 2'-5' oligoadenylate synthetase A inhibits the replication of West Nile virus. *Jpn. J. Vet. Res.* 60, 95–103 (2012).

22. Langevin, S. A., Bunning, M., Davis, B. & Komar, N. Experimental infection of chickens as candidate sentinels for West Nile virus. *Emerg. Infect. Dis.* 7, 726–729 (2001).

23. Balakrishnan, C. N. *et al.* Gene duplication and fragmentation in the zebra finch major histocompatibility complex. *BMC Biol.* 8, 29 (2010).

24. Bean, A. G. D. *et al.* Studying immunity to zoonotic diseases in the natural host - keeping it real. *Nat. Rev. Immunol.* 13, 851–61 (2013).

25. Hofmeister, E. K., Lund, M., Shearn-Bochsler, V. & Balakrishnan, C. N. Susceptibility and Antibody Response of the Laboratory Model Zebra Finch (*Taeniopygia guttata*) to West Nile Virus. *PLoS One* **12,** e0167876 (2017).

26. Warren, W. C. *et al.* The genome of a songbird. *Nature* 464, 757–62 (2010).

27. Hofmeister, E. K., Dusek, R. J., Fassbinder-Orth, C., Owen, B. & Franson, J. C. Susceptibility and antibody response of vesper sparrows (P*ooecetes gramineus*) to West Nile virus: a potential amplification host in sagebrush-grassland habitat. *J. Wildl. Dis.* 52, 2015–06–148 (2016).

28. Love, M. I., Huber, W. & Anders, S. Moderated estimation of fold change and dispersion for RNA-seq data with DESeq2. *Genome Biol.* 15, 550 (2014).

29. Leng, N. *et al.* EBSeq-HMM: A Bayesian approach for identifying gene-expression changes in ordered RNA-seq experiments. *Bioinformatics* 31, 2614–2622 (2015).

30. Wu, X. & Watson, M. CORNA: Testing gene lists for regulation by microRNAs. *Bioinformatics* 25, 832–833 (2009).

31. Benjamini, Y. & Hochberg, Y. Controlling the false discovery rate: a practical and powerful approach to multiple testing. *J. R. Stat. Soc.* 57, 289–300 (1995).

32. Barber, M. R., Aldridge Jr., J. R., Webster, R. G. & Magor, K. E. Association of RIG-I with innate immunity of ducks to influenza. *Proc. Natl. Acad. Sci. U. S. A.* 107, 5913–5918 (2010).

33. Huang, Y. *et al.* The duck genome and transcriptome provide insight into an avian influenza virus reservoir species. *Nat. Genet.* 45, 776–83 (2013).

34. Wei, L. *et al.* Duck MDA5 functions in innate immunity against H5N1 highly pathogenic avian influenza virus infections. *Vet. Res.* 45, 66 (2014).

35. Luo, W. & Brouwer, C. Pathview: An R/Bioconductor package for pathway-based data integration and visualization. *Bioinformatics* 29, 1830–1831 (2013).

36. Grabherr, M. G. *et al.* Full-length transcriptome assembly from RNA-Seq data without a reference genome. *Nat. Biotechnol.* 29, 644–52 (2011).

37. Buchfink, B., Xie, C. & Huson, D. H. Fast and sensitive protein alignment using DIAMOND. *Nat Meth* 12, 59–60 (2015).

38. Huson, D., Mitra, S. & Ruscheweyh, H. Integrative analysis of environmental sequences using MEGAN4. *Genome Res.* 21, 1552–1560 (2011).

39. Takeuchi, O. & Akira, S. Innate immunity to virus infection. *Immunol. Rev.* 227, 75–86 (2009).

40. Fassbinder-Orth, C. A., Barak, V. A., Rainwater, E. L. & Altrichter, A. M. Buggy Creek Virus (Togaviridae: Alphavirus) upregulates expression of pattern recognition receptors and interferons in house sparrows (*Passer domesticus*). *Vector-Borne Zoonotic Dis.* 14, 439–446 (2014).

41. Jemielity, S. *et al.* TIM-family Proteins Promote Infection of Multiple Enveloped Viruses through Virion-associated Phosphatidylserine. *PLoS Pathog.* 9, (2013).

42. Amara, A. & Mercer, J. Viral apoptotic mimicry. *Nat. Rev. Microbiol.* 13, 461–469 (2015).

566 43. Qian, F. *et al.* Identification of Genes Critical for Resistance to Infection by West
567 Nile Virus Using RNA-Seq Analysis. *Viruses* 5, (2013).
568
569 44. Hussmann, K. L. & Fredericksen, B. L. Differential induction of CCL5 by
570 pathogenic and non-pathogenic strains of West Nile virus in brain endothelial cells and
571 astrocytes. *J. Gen. Virol.* 95, 862–867 (2014).
572
573 45. Kumar, M., Belcaid, M. & Nerurkar, V. R. Identification of host genes leading to
574 West Nile virus encephalitis in mice brain using RNA-seq analysis. *Sci. Rep.* 6, 26350
575 (2016).
576
577 46. Venter, M. *et al.* Gene expression in mice infected with West Nile virus strains of
578 different neurovirulence. *Virology* 342, 119–140 (2005).
579
580 47. Schoggins, J. J. W. *et al.* A diverse array of gene products are effectors of the type
581 I interferon antiviral response. *Nature* 472, 481–485 (2011).
582
583 48. Liu, Y., King, N., Kesson, A., Blanden, R. V. & Müllbacher, A. Flavivirus
584 infection up-regulates the expression of class I and class II major histocompatibility
585 antigens on and enhances T cell recognition of astrocytes in vitro. *J. Neuroimmunol.* 21,
586 157–168 (1989).
587
588 49. Lobigs, M., Müllbacher, A. & Lee, E. Evidence that a mechanism for efficient
589 flavivirus budding upregulates MHC class I. *Immunol. Cell Biol.* 82, 184–188 (2004).
590
591 50. Watzl, C. How to trigger a killer: Modulation of natural killer cell reactivity on
592 many levels. *Adv. Immunol.* 124, (Elsevier Inc., 2014).
593
594 51. Kumar, M., Verma, S. & Nerurkar, V. R. Pro-inflammatory cytokines derived
595 from West Nile virus (WNV)-infected SK-N-SH cells mediate neuroinflammatory
596 markers and neuronal death. *J. Neuroinflammation* 7, 73 (2010).
597
598 52. Karim, R. *et al.* Human Papillomavirus (HPV) Upregulates the Cellular
599 Deubiquitinase UCHL1 to Suppress the Keratinocyte's Innate Immune Response. *PLoS*
600 *Pathog.* 9, (2013).
601
602 53. Brass, A. L. *et al.* The IFITM Proteins Mediate Cellular Resistance to Influenza A
603 H1N1 Virus, West Nile Virus, and Dengue Virus. *Cell* 139, 1243–1254 (2009).
604
605 54. Jeurissen, S. H. The role of various compartments in the chicken spleen during an
606 antigen-specific humoral response. *Immunology* 80, 29–33 (1993).
607
608 55. Smith, K. G. & Hunt, J. L. On the use of spleen mass as a measure of avian
609 immune system strength. *Oecologia* 138, 28–31 (2004).
610

611 56. Martin, M. Cutadapt removes adapter sequences from high-throughput
612 sequencing reads. *EMBnet.journal* 17, 10 (2011).
613
614 57. Kim, D. *et al.* TopHat2: accurate alignment of transcriptomes in the presence of
615 insertions, deletions and gene fusions. *Genome Biol.* 14, R36 (2013).
616
617 58. Langmead, B. & Salzberg, S. L. Fast gapped-read alignment with Bowtie 2. *Nat*
618 *Methods* 9, 357–359 (2012).
619
620 59. Li, H. *et al.* The Sequence Alignment/Map format and SAMtools. *Bioinformatics*
621 25, 2078–2079 (2009).
622
623 60. Li, H. A statistical framework for SNP calling, mutation discovery, association
624 mapping and population genetical parameter estimation from sequencing data.
625 *Bioinformatics* 27, 2987–2993 (2011).
626
627 61. Anders, S., Pyl, P. T. & Huber, W. HTSeq-A Python framework to work with
628 high-throughput sequencing data. *Bioinformatics* 31, 166–169 (2015).
629
630 62. R Core Team (2016). R: A language and environment for statistical computing. R
631 Foundation for Statistical Computing, Vienna, Austria. URL https://www.R-project.org/.
632
633 63. Marini F (2016). *pcaExplorer: Interactive Visualization of RNA-seq Data Using a*
634 *Principal Components Approach*. R package version
635 1.1.2, https://github.com/federicomarini/pcaExplorer.
636
637 64. H. Wickham. ggplot2: Elegant Graphics for Data Analysis. Springer-Verlag New
638 York, 2009.
639
640 65. Seyednasrollah, F., Laiho, A. & Elo, L. L. Comparison of software packages for
641 detecting differential expression in RNA-seq studies. *Brief. Bioinform.* 16, 59–70 (2013).
642
643 66. Videvall, E., Cornwallis, C. K., Palinauskas, V., Valkiūnas, G. & Hellgren, O.
644 The avian transcriptome response to malaria infection. *Mol. Biol. Evol.* 32, 1255–67
645 (2015).
646
647 67. Kanehisa, M. & Goto, S. KEGG: Kyoto Encyclopedia of Genes and Genomes.
648 *Nucleic Acids Res.* **28 ,** 27–30 (2000).
649
650 68. Kanehisa, M., Sato, Y., Kawashima, M., Furumichi, M. & Tanabe, M. KEGG as a
651 reference resource for gene and protein annotation. *Nucleic Acids Res.* **44 ,** D457–D462
652 (2016).
653
654 69. Elbahesh, H., Scherbik, S. V. & Brinton, M. A. West Nile virus infection does not
655 induce PKR activation in rodent cells. *Virology* 421, 51–60 (2011).
656

Acknowledgements

The authors wish to thank Melissa Lund for technical assistance. Funding provided by U.S. Geological Survey National Wildlife Health Center and East Carolina University. Any use of trade, firm, or product names is for descriptive purposes only and does not imply endorsement by the U.S. Government

Author Contributions

EKH & CNB conceived the study. EKH performed experimental infections and dissection. CNB & DJN extracted and sequenced RNA and performed data analysis. All authors wrote and approved the manuscript.

Additional Information

Sequencing data have been deposited in the Sequence Read Archive (SRA) under accession PRJNA352507. The authors declare no competing financial interests

700 Table 1. **Candidate immune genes differentially expressed in the present study and**
701 **comparisons with mammals.**
702

Ensembl ID	Gene Name	Log_2 Fold Change	padj	Regulation Pattern Observed	Regulation Pattern in Mammals	Reference
Control vs Infected						
ENSTGUG00000013615	NFKBIZ	0.73	0.064	Up	Up	45
Control vs 2dpi						
ENSTGUG00000000297	IL18	1.01	0.010	Up	No change	51
ENSTGUG00000000678	TIM1	1.49	7.99E-05	Up	Up	41,42
ENSTGUG00000001485	IRF6	-2.09	0.037	Down	Up	43
ENSTGUG00000003354	NKRF	-2.35	4.85E-05	Down	Unknown	
ENSTGUG00000005295	C-C motif chemokine	2.08	0.007	Up	Up	43,44,45
ENSTGUG00000008638	UCHL1	-1.91	0.029	Down	Unknown	
ENSTGUG00000008991	APOD	1.76	0.053	Up	Up	46
ENSTGUG00000009454	IFITM10	1.24	2.71E-04	Down	Unknown	
ENSTGUG00000009769	TNFRSF13C	0.89	0.010	Up	Unknown	
ENSTGUG00000015634	Novel gene (MHC IIB)	2.23	0.001	Up	Up	48
ENSTGUG00000016383	SIGLEC1	1.39	0.046	Up	Up	45
ENSTGUG00000017149	Novel gene (MHC IIB)	1.57	0.099	Up	Up	48
Control vs 4dpi						
ENSTGUG00000001516	DDx58	1.50	1.45E-08	Up	Up	45
ENSTGUG00000002144	IRF4	1.39	0.022	Up	Up	43
ENSTGUG00000002305	LY86	-1.07	1.70E-05	Down	Unknown	
ENSTGUG00000002516	DHx58	1.67	4.05E-06	Up	Up	45
ENSTGUG00000004105	ADAR	1.13	1.70E-05	Up	Up	47
ENSTGUG00000006914	IFIH1	0.95	0.093	Up	Up	45
ENSTGUG00000007454	TNFRSF13B	1.61	0.010	Up	Unknown	
ENSTGUG00000008354	IFIT5	2.97	1.07E-09	Up	Unknown	
ENSTGUG00000008788	EIF2AK2	2.15	9.86E-07	Up	Up	43,69
ENSTGUG00000009162	PXK	1.19	0.011	Up	Unknown	
ENSTGUG00000009536	TRIM25	1.24	0.001	Up	Up	45
ENSTGUG00000009838	IRF7	0.80	0.047	Up	Up	45
ENSTGUG00000011784	ZC3HAV1	1.31	7.09E-08	Up	Up	45
ENSTGUG00000017534	MOV10	1.29	0.017	Up	Up	47
2dpi vs 4dpi						
ENSTGUG00000003354	NKRF	1.70	0.033	Up	Unknown	
ENSTGUG00000005206	ADA	-1.48	0.001	Down	Unknown	
ENSTGUG00000011784	ZC3HAV1	0.82	0.058	Up	Up	45

703

Table 2. **Select immune related gene ontology (GO) categories among DEseq2 significantly differentially expressed genes (adjusted p value < 0.10).**

GO ID	Description	Adjusted Fisher
Control vs 4dpi		
GO:0003727	single-stranded RNA binding	0.009
GO:0032481	positive regulation of type I interferon production	0.010
GO:0045087	innate immune response	0.033
GO:1900245	positive regulation of MDA-5 signaling pathway	0.033
GO:1900246	positive regulation of RIG-I signaling pathway	0.033
GO:0006926	virus-infected cell apoptotic process	0.039
GO:0044319	wound healing, spreading of cells	0.039
GO:0032727	positive regulation of interferon-alpha production	0.049
GO:0002230	positive regulation of defense response to virus by host	0.052
GO:0045088	regulation of innate immune response	0.07
2dpi vs 4dpi		
GO:0050862	positive regulation of T cell receptor signaling pathway	0.042
GO:0002906	negative regulation of mature B cell apoptotic process	0.042
GO:0002686	negative regulation of leukocyte migration	0.042
GO:0045580	regulation of T cell differentiation	0.042
GO:0032481	positive regulation of type I interferon production	0.047
GO:0050870	positive regulation of T cell activation	0.057

Figures:

Figure 1. **Immune genes differentially expressed between day 2 post-inoculation and control** A) Heatmap of expression levels (log transformed read counts) across all treatments of immune genes differentially expressed at 2dpi relative to control. B-D) Expression values (normalized read counts) for three key immune genes and their regulation pattern classification by *EBSeqHMM*. Asterisks represent statistical significance in *DEseq2* analysis after FDR correction (* $p<0.10$, ** $p<0.05$, *** $p<0.01$).

Figure 2. **Immune genes differentially expressed between day 4 post-inoculation and control A)** Heatmap of expression levels (log transformed read counts) across all treatments of immune genes differentially expressed at 4dpi relative to control. B-D) Expression values (normalized read counts) for three key immune genes and their regulation pattern classification by *EBSeqHMM*. Asterisks represent statistical significance in *DEseq2* analysis after FDR correction (* $p<0.10$, ** $p<0.05$, *** $p<0.01$).

Figure 3. Regulation of the zebra finch RLR pathway. Color represents $\log_2$ fold change between Control and 4dpi. Asterisks represent statistical significance in *DEseq2* analysis after FDR correction (* $p<0.10$, ** $p<0.05$, *** $p<0.01$).

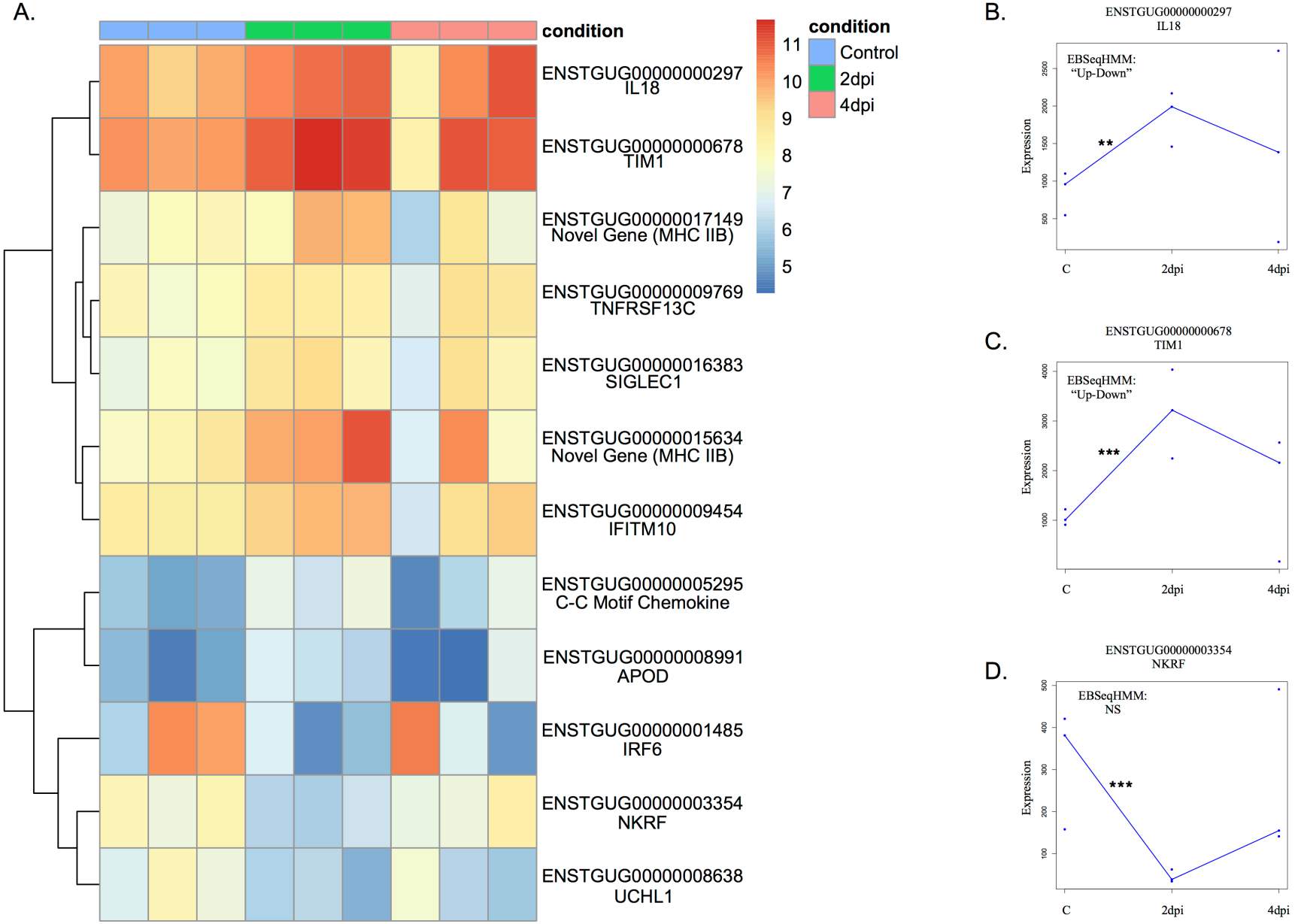

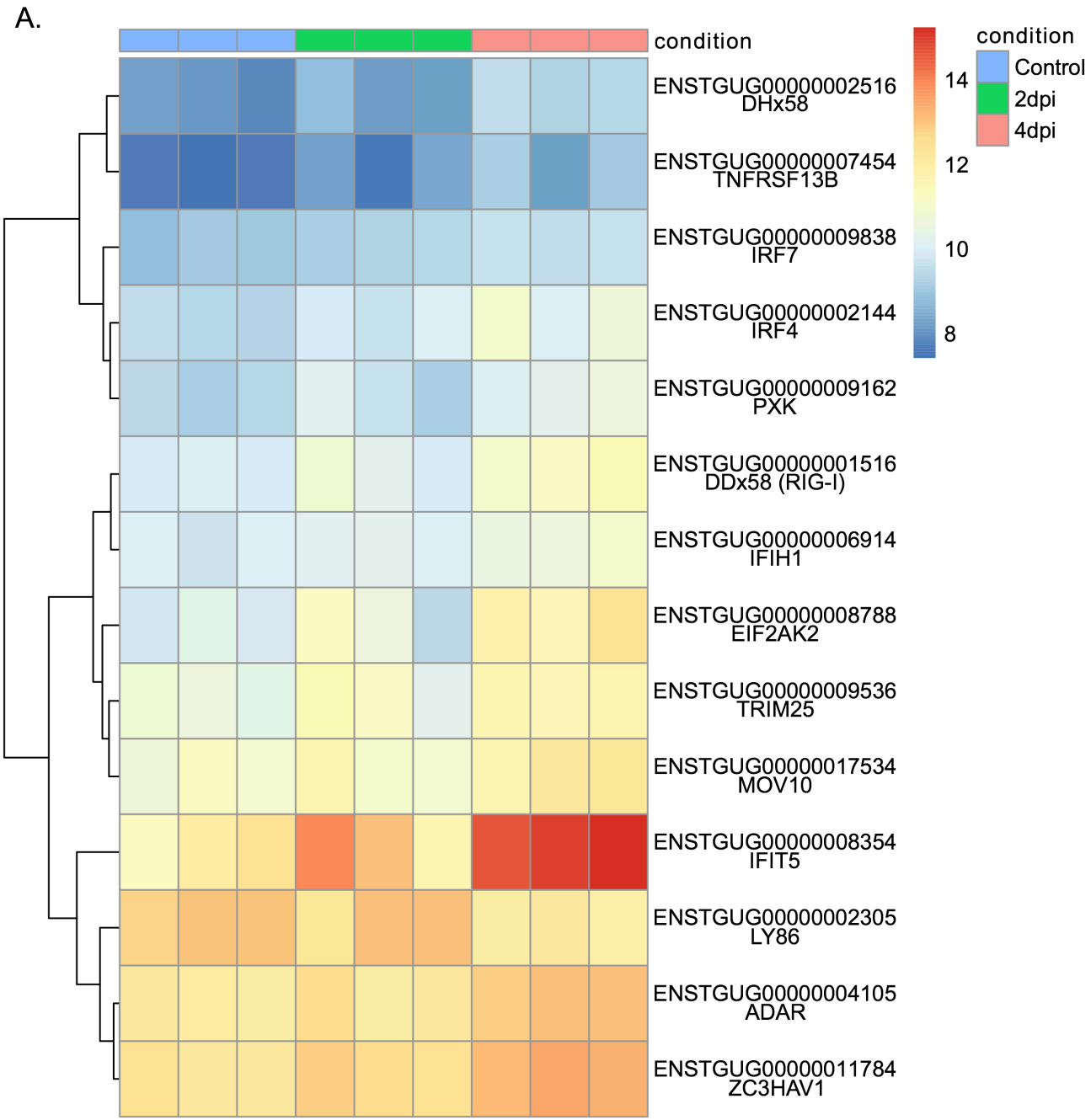

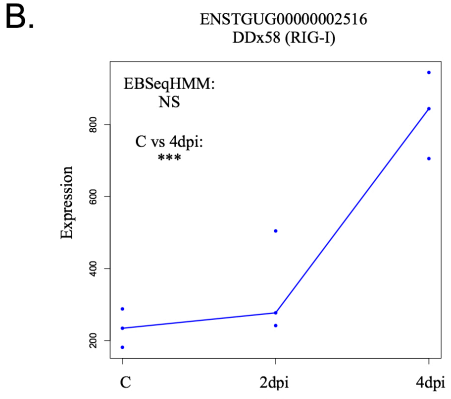

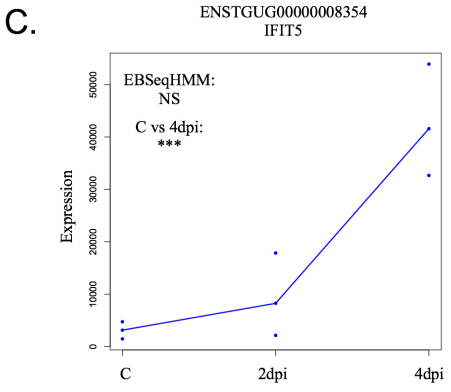

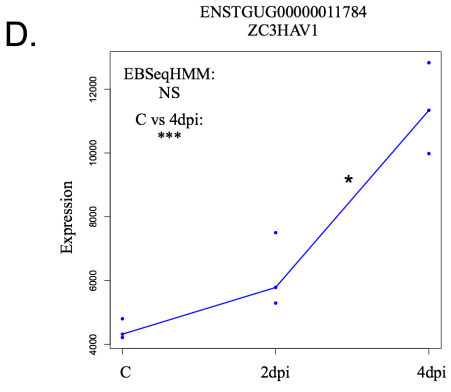

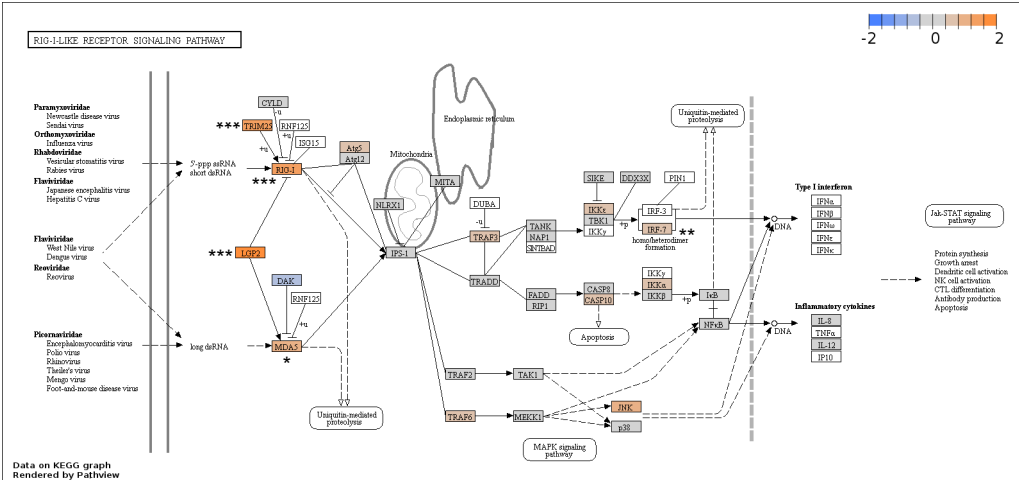
RIG-I-LIKE RECEPTOR SIGNALING PATHWAY
-2
0
2
Paramyxoviridae
Newcastle disease virus
Sendai virus
Orthomyxoviridae
Influenza virus
Rhabdoviridae
Vesicular stomatitis virus
Rabies virus
Flaviviridae
Japanese encephalitis virus
Hepatitis C virus
Flaviviridae
West Nile virus
Dengue virus
Reoviridae
Reovirus
Picornaviridae
Encephalomyocarditis virus
Polio virus
Rhinovirus
Theiler's virus
Mengo virus
Foot-and-mouse disease virus
5'-ppp asRNA
short dsRNA
long dsRNA
CYLD
TRIM25
RNF125
ISG15
RIG-I
Ato5
Atg12
LGP2
DAK
RNF125
MDA5
Endoplasmic reticulum
Mitochondria
MITA
NLRX1
DUBA
IPS-1
TRAF3
TRADD
TANK
NAP1
SINTBA2
FADD
RIP1
CASP8
CASP10
Apoptosis
SIKE
DDX3X
PIN1
IKKε
TBK1
IKKγ
IRF-3
IRF-7
homo/heterodimer
formation
DNA
Type I interferon
IFNα
IFNβ
IFNω
IFNε
IFNκ
Jak-STAT signaling
pathway
Protein synthesis
Growth arrest
Dendritic cell activation
NK cell activation
CTL differentiation
Antibody production
Apoptosis
Ubiquitin-mediated
proteolysis
IKKγ
IKKα
IKKβ
IκB
NFκB
DNA
Inflammatory cytokines
IL-8
TNFα
IL-12
IP10
TRAF2
TAK1
TRAF6
MEKK1
JNK
p38
MAPK signaling
pathway
Ubiquitin-mediated
proteolysis
Data on KEGG graph
Rendered by Pathview